ISSN 1070-3284, Russian Journal of Coordination Chemistry, 2020, Vol. 46, No. 5, pp. 330–338. © Pleiades Publishing, Ltd., 2020.
Russian Text © The Author(s), 2020, published in Koordinatsionnaya Khimiya, 2020, Vol. 46, No. 5, pp. 295–303.

Transformations of Binuclear Iron(II) Pivalate, $Fe_2(\mu\text{-}OOCBu^t)_4(NEt_3)_2$, in the Reactions with Air Oxygen and 3,5-Dimethylpyrazole

M. A. Uvarova[a] and S. E. Nefedov[a, *]

[a] *Kurnakov Institute of General and Inorganic Chemistry, Russian Academy of Sciences, Moscow, 119991 Russia*
**e-mail: snef@igic.ras.ru*

Received October 25, 2019; revised December 9, 2019; accepted December 24, 2019

Abstract—The extraction of a suspension, which is prepared by mixing of iron dichloride, pivalic acid, and triethylamine, with hexane and keeping of the resulting solution at −5°C in a refrigerator result in the formation of single crystals of the binuclear dimeric lantern $Fe_2(\mu\text{-}OOC^tBu)_4(NEt_3)_2$ (**I**). The decantation of the single crystals at room temperature gives an orange product oxidized in air to form a red powder. The dissolution of the powder in a benzene–acetonitrile (10 : 1) mixture in air and the subsequent crystallization give single crystals of complex $\{[Fe_3(\mu^3\text{-}O)(OH_2)(\mu\text{-}OOC^tBu)_5(\eta^2\text{-}OOC^tBu)[O(C^tBu)OHNEt_3)] \cdot MeCN\}$ (**II**). The interaction of the mother liquor with 3,5-dimethylpyrazole (HDmpz) affords complex $Fe_3(\mu^3\text{-}O)(\mu\text{-}OOC^tBu)_6(HDmpz)_3$ (**III**). Complexes **I–III** are characterized by elemental analysis, IR spectroscopy, and X-ray diffraction analysis (CIF files CCDC nos. 1959111 (**I**), 1959112 (**II**), and 1959110 (**III**)).

Keywords: iron(II, III) pivalates, triethylamine, oxidation of iron atoms, trinuclear complexes, pyrazole, synthesis, X-ray diffraction analysis

DOI: 10.1134/S1070328420050085

INTRODUCTION

Binuclear pivalates of 3*d* metals with triethylamine are convenient initial reagents for the study of the proton transfer from the coordinated organic molecule capable of deprotonating, in particular, heterocyclic 3,5-dimethylpyrazole molecules [1–6]. These complexes are characterized by similar structures. On the one hand, they are dimers with the Chinese lantern geometry fairly traditional for the carboxylate chemistry and, on the other hand, their axial position contains the coordinated amine molecule capable of acting as a proton acceptor. Undoubtedly, it is important that these molecules contain no oxygen and hydroxyl bridges, which can also accept hydrogen atoms and mainly determine features of pivalate transformations.

It has previously been shown that the reactions of 3*d*-metal pivalates, regardless of the synthesis methods, with triethylamine afford complexes $M_2(\mu\text{-}OOC^tBu)_4(NEt_3)_2$ (where M = Zn, Cu, Ni, and Co) in an almost quantitative yield. The complexes are highly soluble in various solvents, including saturated organic solvents, and their geometry is determined by the transition metal nature (Table 1). Unlike other 3*d* metals, manganese(II) forms complex $Mn_2(\mu\text{-}OOC^tBu)_4[O(C^tBu)OHNEt_3]_2$ in which the electron-deficient metal atom ($S = 5/2$) is not bound to the nitrogen atom of amine, which donates two electrons to the metal, but is linked with the oxygen atom, being an adduct of pivalic acid and triethylamine capable of additional electron density donating.

When the complex-lanterns were used in the reactions with heterocyclic 3,5-dimethylpyrazole (HDmpz), the deprotonation of pyrazole leading to the pyrazolate-bridged dimers $M_2(\mu\text{-}Dmpz)_2(HDmpz)_2\text{-}(OOC^tBu)_2$ was found for the zinc and cobalt(II) compounds in hexane at room temperature [7, 10]. A mixture of mononuclear $M(HDmpz)_2\text{-}(OOC^tBu)_2$ and binuclear $M_2(\mu\text{-}OOC^tBu)_4(HDmpz)_2$ complexes, whose ratio depends on the nature of the solvent used and crystallization conditions, is formed for copper and nickel, while the $Mn(HDmpz)_4\text{-}(OO^tBu)_2$ monomer was isolated in the case of manganese [8, 9, 11, 12]. The binuclear $Cu_2(\mu\text{-}OOC^tBu)_4(HDmpz)_2$ complex contains the hydrogen bond of the pyrrole NH fragment of the heterocycle with the oxygen atom of the bridging pivalate anion and can be deprotonated by thermolysis at 165°C with pivalic acid removal to form the pyrazolate-bridged dimer isostructural to the zinc and cobalt complexes. In the case of nickel, this bond is absent and the thermolysis of the complexes affords only the Ni_7 cluster containing no pyrazolate anions [12, 13].

In this work, the considered approach is accomplished to obtain the iron(II) pivalate complex $Fe_2(\mu\text{-}$

Table 1. Geometry of the $M_2(\mu\text{-}OOC^tBu)_4(NEt_3)_2$ complexes

Metal	M···M	M–O	M–N	MMN	References
Zn(II)	3.0001(8)	2.034(1)–2.045(1)	2.112(1)	177.5	7
Cu(II)	2.681(1)	1.963(4)–1.967(4)	2.300(4)	177.7	8
Ni(II)	2.778(2)	2.004(5)–2.023(5)	2.106(6)	177.7	9
Co(II)	2.7588(9)	2.019(2)–2.033(2)	2.165(2)	178.3	10
Mn(II)	3.1089(8)	2.054(9)–2.179(9)	2.044(3) (M–O) ←O(C^{t}Bu)O(H)NEt$_3$	177.9	11

$OOC^tBu)_4(NEt_3)_2$ and the structures of the products of its reactions with air oxygen and HDmpz are discussed.

Note that iron(II, III) carboxylates bearing coordinated heterocyclic molecules (pyrazole or imidazole and their analogs) are often considered as structural analogs of the active moiety of natural metalloenzymes responsible for diverse catalytic processes [14–17].

EXPERIMENTAL

All procedures on the synthesis and isolation of the complexes, except for specially indicated cases, were carried out in pure argon using anhydrous solvents.

Synthesis of complexes $Fe_2(\mu\text{-}OOC^tBu)_4(NEt_3)_2$ (I), {[$Fe_3(\mu^3\text{-}O)(OH_2)(\mu\text{-}OOC^tBu)_5(\eta^2\text{-}OOC^tBu)$[O-(C^{t}Bu)OHNEt$_3$)] · MeCN} (II), and $Fe_3(\mu^3\text{-}O)(\mu\text{-}OOC^tBu)_6(HDmpz)_3$ (III). A mixture of iron dichloride (0.2 g, 1.2 mmol) and triethylamine (1 mL, 7.1 mmol) was stirred for 0.5 h. Pivalic acid (0.39 g, 3.8 mmol) was added to the obtained mixture, and stirring was continued at room temperature for 1 h. A green-brown suspension was dissolved in a benzene–heptane (1 : 20) mixture on reflux for 1 h, cooled to room temperature, filtered from a white precipitate, and concentrated on reflux in an oil bath in an argon flow to a volume of 5 mL. The resulting solution was kept at –5°C in a refrigerator for 24 h. The yellow-green crystals formed were decanted from the mother liquor, washed with cold hexane, and dried in an argon flow. The color of the crystals gradually changed to orange during this procedure. The yield of complex **I** was 0.026 g (12%). At room temperature the crystals are transformed into an orange powder. In air the orange powder is instantly transformed into complex **II**.

The yellow-green single crystals of complex **I** suitable for X-ray diffraction (XRD) analysis were isolated directly from a cold mother liquor and rapidly transferred to a diffractometer into a vaporizing nitrogen flow.

In the absence of argon, the orange color of the powder nearly instantly changed to red. The obtained powder was washed with cold hexane (10 mL), dissolved on heating to 50°C in a benzene–acetonitrile (10 : 1) mixture (5 mL), concentrated to 3 mL, and kept at 5°C in a refrigerator. The red crystals of formed complex **II** were separated from the solution by decantation, washed consequently with benzene (5 mL) and hexane (5 mL), and dried in an argon flow. The yield of complex **II** was 0.002 g (4.7%).

For $C_{43}H_{84}N_2O_{16}Fe_3$

Anal. calcd., %	C, 49.06	H, 8.04	N, 2.66
Found, %	C, 48.62	H, 7.95	N, 2.47

IR for **II** (ν, cm^{-1}): 3456 w, 2880 s.br, 2808 m, 2676 s, 2520 m, 2352 w, 100 w, 1652 w, 1628 w, 1476 s, 1444 s, 1396 s, 1364 m, 1332 w, 1288 w, 1172 s, 1072 m, 1036 s, 852 m, 808 m, 760 w, 620 w, 460 w.

The red mother liquor was added with HDmpz (0.15 g, 1.6 mmol), and the mixture was stirred on reflux for 1 h. The solvent was removed to dryness on reflux in an argon flow. The powder was washed with hexane (10 mL) and dissolved in a benzene–acetonitrile (10 : 1) mixture (10 mL). The red-brown solution was concentrated to 5 mL and kept at 5°C in a refrigerator. The brown crystals formed were decanted from the solution, sequentially washed with cold benzene (10 mL) and hexane (10 mL), and dried in an argon flow. The yield of complex **III** was 0.16 g (37%).

For $C_{45}H_{75}N_6O_{13}Fe_3$

Anal. calcd., %	C, 50.25	H, 7.03	N, 7.81
Found, %	C, 49.12	H, 6.95	N, 7.68

IR (KBr; ν, cm^{-1}): 3648 w, 2964 s, 2932 s, 2872 m, 2352 w, 1692 s, 1608 s, 1560 s, 1536 s, 1484 s, 1424 s, 1456 m, 1404 s, 1380 s, 1332 m, 1260 w, 1228 s, 1204 m, 1096 w, 1032 w, 940 w, 900 w, 872 w, 788 m, 652 w, 604 s, 536 w, 444 m.

Table 2. Crystallographic parameters and structure refinement details for complexes **I–III**

Parameter	Value		
	I	**II**	**III**
Empirical formula	$C_{32}H_{66}Fe_2N_2O_8$	$C_{43}H_{84}N_2O_{16}Fe_3$	$C_{45}H_{75}N_6O_{13}Fe_3$
FW	718.57	1052.67	1075.66
Color	Yellow-green	Red	Brown
Crystal system	Monoclinic	Monoclinic	Trigonal
Space group	$P2_1/c$	$P2_1/n$	$R3m$
a, Å	10.1191(14)	12.6314(8)	35.9865(12)
b, Å	17.453(2)	25.2627(15)	35.9865(12)
c, Å	12.0964(17))	17.9889(10)	14.0825(11)
α, deg	90	90	90
β, deg	111.396(3)	103.8840(10)	90
γ, deg	90	90	120
V, Å^3	1989.1(5)	5572.6(6)	15793.9(16)
Z	2	4	9
ρ_{calc}, mg/m^3	1.200	1.255	1.018
μ, mm^{-1}	0.773	0.831	0.660
F(000)	776	2248	5121
Crystal size, mm	0.22 × 0.20 × 0.18	0.24 × 0.22 × 0.20	0.24 × 0.22 × 0.20
Scan range over θ, deg	2.15–30.00	1.61–30.00	2.36–28.99
Ranges of reflection indices	$-13 \le h \le 14$, $-24 \le k \le 21$, $-16 \le l \le 17$	$-17 \le h \le 17$, $-17 \le k \le 35$, $-25 \le l \le 17$	$-38 \le h \le 21$, $-46 \le k \le 19$, $-18 \le l \le 5$
Number of measured reflections	15524	36298	9042
Number of independent reflections (R_{int})	5791 (0.0373)	16047 (0.0431)	4556 (0.0398)
GOOF	1.165	1.007	0.827
R_1, wR_2 ($I > 2\sigma(I)$)	0.0543, 0.1157	0.0746, 0.1649	0.0346, 0.0686
R_1, wR_2 (for all reflections)	0.0898, 0.1229	0.1289, 0.1826	0.0551, 0.0733
Residual electron density (max/min), e Å^{-3}	0.930/–0.321	2.414/–1.484	0.376/–0.213

The IR spectra of the crystalline samples were recorded in a range of 4000–550 cm^{-1} (KBr pellets) on a NEXUS FT-IR spectrometer (NICOLET) using a MIRacle accessory (PIKETechnologies) with the diamond crystal.

XRD analyses of complexes I–III were carried out using a standard procedure on a Bruker SMART Apex II automated diffractometer equipped with a CCD detector (MoK_α, λ = 0.71073 Å, graphite monochromator, ω scan mode) at T = 150 K. The structures were calculated using the SHELXTL PLUS program package (PC version). Structure refinement was performed using the SHELXTL-97 program [18–21]. The solvate molecule of acetonitrile in complex **III** was disordered over several positions and removed from the refinement by the SQUEEZE program [21]. The crystallographic data and structure refinement details are presented in Table 2. Selected geometric parameters of the studied complexes are given in Tables 3–5.

The full tables of atomic coordinates, bond lengths, and bond angles were deposited with the Cambridge Crystallographic Data Centre (CIF files CCDC nos. 1959111 (**I**), 1959112 (**II**), and 1959110 (**III**); deposit@ccdc.cam.ac.uk or http://www.ccdc.cam.ac.uk/data_request/cif).

Table 3. Selected bond lengths and bond angles in complex **I***

Bond	*d*, Å	Bond	*d*, Å
Fe(1)–O(4)	2.0495(19)	Fe(1)–O(2)	2.0507(18)
Fe(1)–O(3)	2.0545(18)	Fe(1)–O(1)	2.0552(19)
Fe(1)–N(1)	2.193(2)	Fe(1)–Fe(1)$^{\#1}$	2.8614(7)
Angle	ω, deg	Angle	ω, deg
O(4)Fe(1)O(2)	88.25(8)	O(4)Fe(1)O(3)	161.32(8)
O(2)Fe(1)O(3)	89.14(8)	O(4)Fe(1)O(1)	89.31(9)
O(2)Fe(1)O(1)	161.89(8)	O(3)Fe(1)O(1)	87.46(8)
O(4)Fe(1)N(1)	100.06(8)	O(2)Fe(1)N(1)	98.34(8)
O(3)Fe(1)N(1)	98.61(8)	O(1)Fe(1)N(1)	99.75(8)
O(4)Fe(1)Fe(1)$^{\#1}$	81.61(6)	O(2)Fe(1)Fe(1)$^{\#1}$	79.65(6)
O(3)Fe(1)Fe(1)$^{\#1}$	79.72(6)	O(1)Fe(1)Fe(1)$^{\#1}$	82.24(6)
N(1)Fe(1)Fe(1)$^{\#1}$	177.38(6)	C(1)O(1)Fe(1)	125.05(18)
C(1)$^{\#1}$O(2)Fe(1)	128.60(18)	C(6)O(3)Fe(1)	128.80(18)
C(6)$^{\#1}$O(4)Fe(1)	126.17(18)	C(15)N(1)Fe(1)	108.21(15)
C(11)N(1)Fe(1)	108.47(15)		

* Symmetry transforms used for the generation of equivalent atoms: $^{\#1}$ $-x + 2, -y, -z + 2$.

RESULTS AND DISCUSSION

It is found that the extraction of the suspension obtained by mixing of iron dichloride, triethylamine, and pivalic acid (room temperature, stirring, 1 h) with hexane results in the formation of a green-brown solution from which very unstable on heating yellow-green single crystals of the binuclear complex $Fe_2(\mu\text{-}OOC^tBu)_4(NEt_3)_2$ (**I**) were obtained at –5°C in a yield of 12%.

According to the XRD data, centrosymmetric complex **I** (Tables 2, 3; Fig. 1a) is a traditional dimer-lantern for the metal pivalates with Et_3N (Table 1) in which the metal atoms exist at a nonbonding Fe···Fe distance of 2.8614(7) Å and are connected by four bridging pivalate anions (Fe–O 2.0495(19)–2.0552(19) Å). The axial position of each metal atom contains coordinated triethylamine molecules (Fe–N 2.193(2) Å). The crystals of complex **I** are very unstable and at room temperature are transformed into an orange compound, which is possibly the trinuclear complex $Fe_3(\mu\text{-}OOC^tBu)_6(NEt_3)_2$ by analogy to the transformations $M_2 \rightarrow M_3$ found for cobalt(II) pivalates with triethylamine (color change from green to violet at room temperature for 10 h) or manganese(II) (thermal heating to 145°C) [10, 11].

The orange powder is instantly oxidized in air to form red crystals of the $\{[Fe_3(\mu^3\text{-}O)(OH_2)(\mu\text{-}OOC^tBu)_5(\eta^2\text{-}OOC^tBu)[O(C^tBu)OHNEt_3)] \cdot MeCN\}$ complex (**II**).

In trinuclear complex **II** (Tables 2, 4; Fig. 1b), three iron atoms (Fe(1)···Fe(2) 3.2634(8), Fe(1)···Fe(3) 3.3127(8), Fe(2)···Fe(3) 3.2861(8) Å) are linked by the tridentate-bridging oxygen atom (Fe(1)–O(1) 1.831(3), Fe(2)–O(1) 2.059(3), Fe(3)–O(1) 1.842(3) Å). Such a substantial difference in the metal–oxygen distances shows that the Fe(1) and Fe(3) atoms are in the oxidation state +3, which is confirmed by the distribution of bond lengths with the oxygen atoms of the bridging pivalate anions (Fe(1)–O 1.972(3)–2.044(3), Fe(3)–O 1.983(3)–2.026(3) Å), which are noticeably shortened compared to similar distances for the Fe(2) atom in the oxidation state +2 (Fe(2)–O 2.102(3)–2.149(3) Å). The distorted octahedral environment of the Fe(1) atom was supplemented by the oxygen atom of the terminal adduct $\leftarrow O(C^tBu)O(H)NEt_3$ (Fe(1)–O(7) 2.044(3), N(1)···O(6) 2.737(4) Å). Note that the same adduct was observed in the axial position of the $Mn_2(\mu\text{-}OOC^tBu)_4[O(C^tBu)O(H)NEt_3]_2$ complex obtained by the reaction of manganese(II) pivalate with triethylamine [11]. The distorted octahedron of the Fe(3) atom is supplemented by the oxygen atoms of the η^2-pivalate anion (Fe(3)–O 2.063(3), 2.227(3) Å), whereas that of the Fe(2) atom is supplemented by the

Table 4. Selected bond lengths and bond angles in complex **II**

Bond	*d*, Å	Bond	*d*, Å
Fe(1)–O(1)	1.831(3)	Fe(1)–O(4)	1.972(3)
Fe(1)–O(2)	2.022(3)	Fe(1)–O(10)	2.027(3)
Fe(1)–O(7)	2.044(3)	Fe(2)–O(1)	2.059(3)
Fe(2)–O(12)	2.102(3)	Fe(2)–O(5)	2.110(3)
Fe(2)–O(16)	2.112(3)	Fe(2)–O(3)	2.149(3)
Fe(2)–O(9)	2.158(3)	Fe(3)–O(1)	1.842(3)
Fe(3)–O(13)	1.983(3)	Fe(3)–O(11)	2.022(3)
Fe(3)–O(8)	2.026(3)	Fe(3)–O(14)	2.063(3)
Fe(3)–O(15)	2.227(3)		
Angle	ω, deg	Angle	ω, deg
O(1)Fe(1)O(4)	108.21(12)	O(1)Fe(1)O(2)	98.12(12)
O(4)Fe(1)O(2)	90.00(13)	O(1)Fe(1)O(10)	98.30(12)
O(4)Fe(1)O(10)	87.20(12)	O(2)Fe(1)O(10)	163.39(12)
O(1)Fe(1)O(7)	102.19(12)	O(4)Fe(1)O(7)	149.58(12)
O(2)Fe(1)O(7)	86.83(12)	O(10)Fe(1)O(7)	87.32(12)
O(1)Fe(2)O(12)	92.96(11)	O(1)Fe(2)O(5)	92.86(11)
O(12)Fe(2)O(5)	88.44(13)	O(1)Fe(2)O(16)	176.56(11)
O(12)Fe(2)O(16)	83.73(12)	O(5)Fe(2)O(16)	86.15(12)
O(1)Fe(2)O(3)	93.43(10)	O(12)Fe(2)O(3)	173.56(12)
O(5)Fe(2)O(3)	90.45(12)	O(16)Fe(2)O(3)	89.87(12)
O(1)Fe(2)O(9)	92.96(10)	O(12)Fe(2)O(9)	93.53(12)
O(5)Fe(2)O(9)	173.76(11)	O(16)Fe(2)O(9)	88.18(11)
O(3)Fe(2)O(9)	86.93(11)	O(1)Fe(3)O(13)	104.19(12)
O(1)Fe(3)O(11)	96.98(12)	O(13)Fe(3)O(11)	86.63(14)
O(1)Fe(3)O(8)	98.16(12)	O(13)Fe(3)O(8)	92.63(13)
O(11)Fe(3)O(8)	164.55(12)	O(1)Fe(3)O(14)	100.78(12)
O(13)Fe(3)O(14)	154.80(12)	O(11)Fe(3)O(14)	87.07(14)
O(8)Fe(3)O(14)	87.09(12)	O(1)Fe(3)O(15)	161.48(11)
O(13)Fe(3)O(15)	94.23(11)	O(11)Fe(3)O(15)	81.98(12)
O(8)Fe(3)O(15)	82.69(11)	O(14)Fe(3)O(15)	60.72(11)
O(1)Fe(3)C(31)	131.32(14)	O(13)Fe(3)C(31)	124.36(14)
O(11)Fe(3)C(31)	83.49(14)	O(8)Fe(3)C(31)	84.21(13)
O(14)Fe(3)C(31)	30.54(13)	O(15)Fe(3)C(31)	30.18(12)
Fe(1)O(1)Fe(3)	128.80(15)	Fe(1)O(1)Fe(2)	113.89(13)
Fe(3)O(1)Fe(2)	114.62(13)	C(1)O(2)Fe(1)	135.7(3)
C(1)O(3)Fe(2)	125.8(3)	C(6)O(4)Fe(1)	123.3(3)
C(6)O(5)Fe(2)	139.3(3)	C(11)O(7)Fe(1)	100.1(3)
C(16)O(8)Fe(3)	135.1(3)	C(16)O(9)Fe(2)	129.1(3)
C(21)O(10)Fe(1)	131.7(3)	C(21)O(11)Fe(3)	133.2(3)
C(26)O(12)Fe(2)	136.0(3)	C(26)O(13)Fe(3)	127.0(3)
C(31)O(14)Fe(3)	93.4(3)	C(31)O(15)Fe(3)	86.2(3)

Table 5. Selected bond lengths and bond angles in complex **III***

Bond	*d*, Å	Bond	*d*, Å
Fe(1)–O(1)	1.955(3)	Fe(1)–O(2)	2.058(3)
Fe(1)–O(7)	2.068(3)	Fe(1)–N(1)	2.145(4)
Fe(1)–O(2)$^{\#1}$	2.058(3)	Fe(1)–O(7)$^{\#1}$	2.068(3)
Fe(2)–O(1)	1.869(2)	Fe(2)–O(3)	2.015(3)
Fe(2)–O(4)	2.038(3)	Fe(2)–O(5)	2.046(3)
Fe(2)–O(6)	2.047(3)	Fe(2)–N(3)	2.194(3)
Angle	**ω, deg**	**Angle**	**ω, deg**
O(1)Fe(1)O(2)	93.42(12)	O(1)Fe(1)O(7)	93.86(11)
O(1)Fe(1)N(1)	175.47(13)	O(1)Fe(1)O(2)$^{\#1}$	93.42(11)
O(1)Fe(1)O(7)$^{\#1}$	93.86(10)	O(2)Fe(1)O(7)	172.65(12)
O(2)Fe(1)N(1)	89.97(13)	O(2)Fe(1)O(2)$^{\#1}$	83.11(12)
O(2)Fe(1)O(7)$^{\#1}$	97.46(12)	O(7)Fe(1)N(1)	82.71(13)
O(2)$^{\#1}$Fe(1)O(7)	97.46(12)	O(7)Fe(1)O(7)$^{\#1}$	81.04(11)
O(2)$^{\#1}$Fe(1)N(1)	89.97(12)	O(7)$^{\#1}$Fe(1)N(1)	82.71(12)
O(2)$^{\#1}$Fe(1)O(7)$^{\#1}$	172.65(12)	O(1)Fe(2)O(3)	95.52(12)
O(1)Fe(2)O(4)	96.18(12)	O(1)Fe(2)O(5)	96.25(11)
O(1)Fe(2)O(6)	96.18(13)	O(1)Fe(2)N(3)	176.52(12)
O(3)Fe(2)O(4)	95.61(12)	O(3)Fe(2)O(5)	88.50(12)
O(3)Fe(2)O(6)	168.21(13)	O(3)Fe(2)N(3)	85.92(12)
O(4)Fe(2)O(5)	166.48(12)	O(4)Fe(2)O(6)	84.58(12)
O(4)Fe(2)N(3)	80.51(13)	O(5)Fe(2)O(6)	88.79(12)
O(5)Fe(2)N(3)	86.96(13)	O(6)Fe(2)N(3)	82.48(12)
Fe(1)O(1)Fe(2)	119.42(11)	Fe(1)O(1)Fe(2)$^{\#1}$	119.42(12)
Fe(2)O(1)Fe(2)$^{\#1}$	121.12(14)	Fe(1)O(2)C(1)	131.0(3)
Fe(2)O(3)C(1)	131.4(3)	Fe(2)O(4)C(6)	132.2(3)
Fe(2)O(5)C(11)	131.8(3)	Fe(2)O(6)C(16)	132.5(3)
Fe(1)O(7)C(6)$^{\#1}$	132.4(3)	Fe(1)N(1)N(2)	113.9(3)
Fe(1)N(1)C(20)	139.3(3)		

* Symmetry transforms used for the generation of equivalent atoms: $^{\#1}$ $-x + 1, -y + 1, z$.

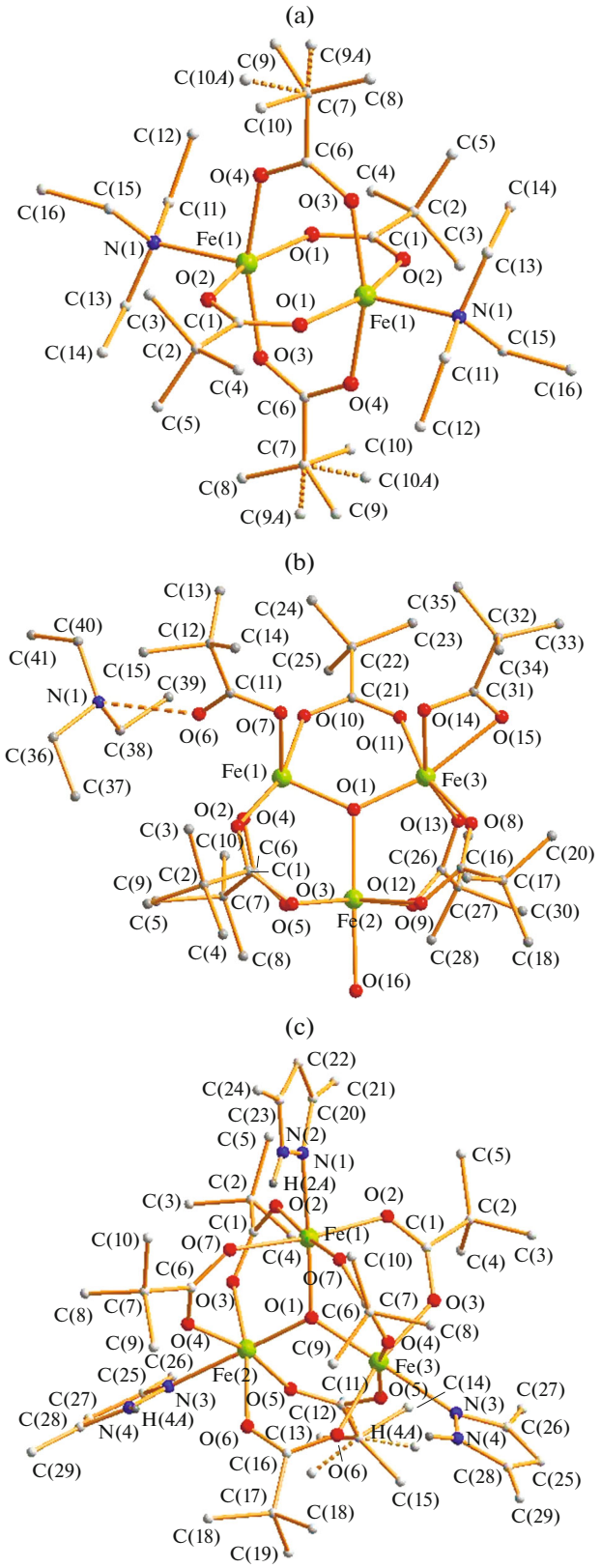

Fig. 1. Structures of complexes (a) **I**, (b) **II**, and (c) **III**.

oxygen atom of the coordinated water molecule (Fe(2)–O 2.112(3) Å). The hydrogen atoms of the water molecule form hydrogen bonds with the oxygen atoms of the bridging pivalate anions of the adjacent Fe_3 molecule (O···O 2.745(6)–2.884(6) Å) to produce dimers in the crystal cell. Solvate molecules of polar donating acetonitrile are arranged above and below the dimers and have no appreciable contacts (Fig. 2a).

The interaction of the mother liquor, which was obtained after the single crystals of complex **I** were isolated, with HDmpz excess in air affords complex $Fe_3(\mu^3\text{-}O)(\mu\text{-}OOC^tBu)_6(HDmpz)_3$ (**III**) in a yield of 37% (Tables 2, 5; Fig. 1c). According to the XRD data, similarly to complex **II**, complex **III**, whose molecule exists in the partial position and the Fe(2) and Fe(2*A*) atoms are arranged symmetrically, contains the oxygen atom bound via the tridentate mode (Fe(1)–O(1) 1.955(3), Fe(2)–O(1) 1.8687(17) Å), and all iron atoms are linked pairwise by two pivalate bridges (Fe(1)–O 2.058(3)–2.068(3), Fe(2)–O 2.015(3)–2.047(3) Å). The distribution of the M–O bond lengths in the complex shows that the Fe(1) atom has the oxidation state +2 and the Fe(2) atoms are in the oxidation state +3. Each iron atom in the complex is coordinated by the pyrazole molecule (Fe(1)–N 2.145(5), Fe(2)–N 2.194(3) Å) and has a distorted octahedral environment, and the pyrrole NH fragments of HDmpz form hydrogen bonds with the oxygen atoms of the bridging anions (N···O 2.744(5)–2.944(6) Å). In the crystal the molecules are packed into piles, and the crystal has pores ($d \approx 3$ Å). However, no solvate guest molecules were observed in the pores (Fig. 2b).

Thus, although the pivalate-bridged dimer of iron(II) containing the proton acceptor was obtained, its reaction with pyrazole affords no pyrazolate-bridged complexes by analogy to the zinc(II), copper, and cobalt(II) complexes. The final products are the traditional stable trinuclear iron(II, III) complexes containing the tridentate-bridging oxygen atoms formed due to the oxidation of iron pivalates with air oxygen [22, 23]. It should be mentioned that the hexanuclear cluster $\{[Fe_3(\mu^3\text{-}O)(\mu\text{-}OOC^tBu)_4(OOC^tBu)_2(HDmpz)(\mu,\eta^5\text{-}Dmpz)(\mu\text{-}K)]_2 \cdot 2HDmpz\}$ is presently the single structurally characterized pyrazolate-bridged iron complex with carboxylate anions [23]. The studies of the possibility of the deprotonation of pyrazole and its analogs in the presence of iron carboxylates are being continued.

ACKNOWLEDGMENTS

The XRD and IR studies of the complexes were carried out using the equipment of the Center for Collective Use of Physical Methods of Investigation at the Kurnakov Institute of General and Inorganic Chemistry (Russian Academy of Sciences) supported by the state task in the area of basic

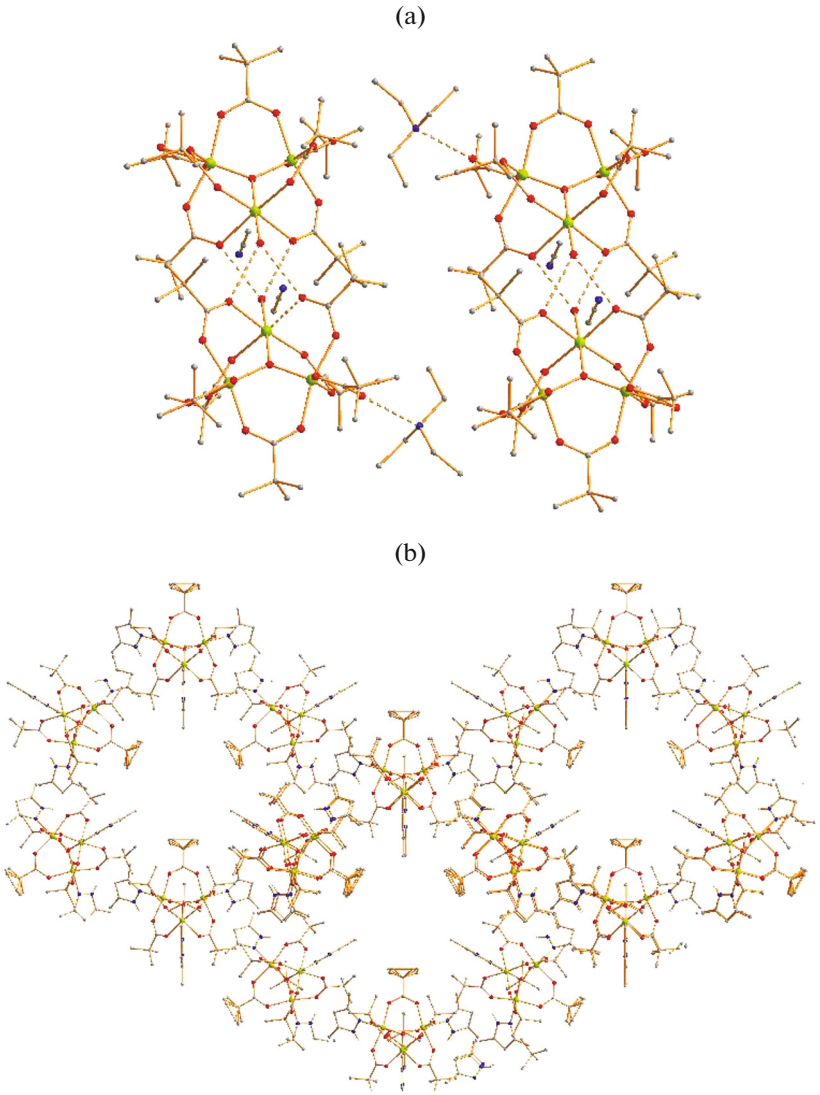

Fig. 2. Packing fragment of molecules of complexes (a) **II** and (b) **III** in the crystal. The dimeric fragments formed due to hydrogen bonds of the coordinated water molecules are shown in complex **II**. The atoms are colored as follows: iron is light green, oxygen is red, nitrogen is blue, and carbon is gray.

research of the Kurnakov Institute of General and Inorganic Chemistry (Russian Academy of Sciences).

FUNDING

This work was supported by the state task in the area of basic research of the Kurnakov Institute of General and Inorganic Chemistry (Russian Academy of Sciences).

CONFLICT OF INTEREST

The authors declare that they have no conflicts of interest.

REFERENCES

1. Halcrow, M.A., *Dalton Trans.*, 2009, p. 2059. https://doi.org/10.1039/B815577A
2. Cingolani, A., Galli, S., Masciocchi, N., et al., *J. Am. Chem. Soc.*, 2005, vol. 127, p. 6144. https://doi.org/10.1021/ja050856+
3. Masciocchi, N., Ardizzoia, G.A., Brenna, S., et al., *Inorg. Chem.*, 2002, vol. 41, p. 6080. https://doi.org/10.1021/ic025821e
4. Cingolani, A., Galli, S., Masciocchi, N., et al., *Dalton Trans.*, 2006, p. 2486. https://doi.org/10.1039/B515630K
5. Miras, H.N., Zhao, H., Herchel, R., et al., *Eur. J. Inorg. Chem.*, 2008, p. 4745. https://doi.org/10.1002/ejic.200800349

6. Nefedov, S.E., *Russ. J. Inorg. Chem*., 2006, vol. 51, suppl. 1, p. S49. https://doi.org/10.1134/S0036023606130031
7. Amel'chenkova, E.V., Denisova, T., and Nefedov, S.E., *Russ. J. Inorg. Chem.,* 2006, vol. 51, no. 8, p. 1218. https://doi.org/10.1134/s0036023606080110
8. Mikuriya, M., Azuma, H., Nukada, R., and Handa, M., *Chem. Lett.*, 1999, vol. 8, p. 57. https://doi.org/10.1246/cl.1999.57
9. Denisova, T.O., Alexandrov, G.G., Fialkovsky, O.P., and Nefedov, S.E., *Russ. J. Inorg. Chem.,* 2003, vol. 48, no. 9, p. 1340.
10. Denisova, T.O., Dobrokhotova, Z.B., Ikorskii, V.N., et al., *Russ. J. Inorg. Chem.,* 2006, vol. 51, no. 9, p. 1363. https://doi.org/10.1134/s0036023606090051
11. Amel'chenkova, E.V., Denisova, T.O., and Nefedov, S.E., *Mendeleev Commun.*, 2004, vol. 14, no. 3, p. 103. https://doi.org/10.1070/MC2004v014n03ABEH001918
12. Denisova, T.O., Amel'chenkova, E.V., Pruss, I.V., et al., *Russ. J. Inorg. Chem.,* 2006, vol. 51, no. 7, p. 1020. https://doi.org/10.1134/s0036023606070084
13. Amel'chenkova, E.V., Denisova, T.O., and Nefedov, S.E., *Russ. J. Inorg. Chem.,* 2006, vol. 51, no. 11, p. 1763. https://doi.org/10.1134/s0036023606110131
14. Lippard, S.J. and Berg, J.M., *Principles of Bioinorganic Chemistry*, Mill Valley: Univ. Science Books, 1994.
15. Solomon, E.I., Sundaram, U.M., and Machonkin, T.E., *Chem. Rev.*, 1996, vol. 96, p. 2563. https://doi.org/10.1021/cr950046o
16. Holm, R.H., Kennepohl, P., and Solomon, E.I., *Chem. Rev.*, 1996, vol. 96, p. 2239. https://doi.org/0.1021/cr9500390
17. Eady, R.R., *Coord. Chem. Rev.*, 2003, p. 237. https://doi.org/10.1016/S0010-8545(02)00248-5
18. *SMART (control) and SAINT (integration) Software. Version 5.0*, Madison: Bruker AXS Inc., 1997.
19. *SAINT: Area-Detector Integration Sofware,* Madison, Bruker AXS Inc., 2012.
20. Sheldrick, G.M., *SADABS. Program for Scaling and Correction of Area Detector Data*, Göttingen: Univ. of Göttingen, 1997.
21. Sheldrick, G.M., *Acta Crystallogr., Sect. C: Struct. Chem.*, 2015, vol. 71, p. 3. https://doi.org/10.1107/S2053229614024218
22. Kiskin, M.A. and Eremenko, I.L., *Russ. Chem. Rev.*, 2006, vol. 75, p. 559. https://doi.org/10.1070/RC2006v075n07ABEH003636
23. Uvarova, M.A. and Nefedov, S.E., *Russ. J. Coord. Chem.*, 2020, vol. 46, no. 2, p. 105. https://doi.org/10.1134/S1070328420020074

Translated by E. Yablonskaya